Hydrocoel Morphogenesis Forming the Pentaradial Body Plan in a Sea Cucumber, *Apostichopus Japonicus*

Sumio Udagawa
University of Tokyo
Takafumi Ikeda
University of Tokyo
Kohei Oguchi
National Institute of Advanced Industrial Science and Technology
Hisanori Kohtsuka
University of Tokyo
Toru Miura (miu@mmbs.s.u-tokyo.ac.jp)
University of Tokyo

Research Article

Keywords: Hydrocoel morphogenesis, pentaradial body plan, sea cucumber, Apostichopus japonicus, Echinoderms constitute, animal phylum, developmental mechanism

Posted Date: December 10th, 2021

DOI: https://doi.org/10.21203/rs.3.rs-1136293/v1

Version of Record: A version of this preprint was published at Scientific Reports on April 11th, 2022. See the published version at https://doi.org/10.1038/s41598-022-09691-y.

Abstract

Echinoderms constitute an animal phylum characterized by the pentaradial body plan. During the development from bilateral larvae to pentaradial adults, the formation of the multiple of five hydrocoel lobes, i.e., the buddings from the mesodermal coelom, is the firstly emerging pentameral character. The developmental mechanism underlying the hydrocoel-lobe formation should be revealed to understand the evolutionary process of this unique and highly derived body plan of echinoderms, although the morphogenetic mechanisms of hydrocoel lobes is largely uninvestigated. In this study, using the sea cucumber *Apostichopus japonicus,* in which the hydrocoel is easily observable, the developmental process of hydrocoel lobes was described in detail, focusing on the cell proliferation and rearrangement. Cell proliferation was not specifically distributed in the growing tips of the hydrocoel lobes and inhibition of the cell proliferation did not affect the lobe formation. During lobe formation, epithelium of the hydrocoel lobes were firstly stratified and then transformed into single-layered, suggesting that radial cell intercalation contributes to hydrocoel-lobe formation.

Introduction

Species belonging to the phylum Echinodermata constitute a deuterostome clade that shows unique pentaradial body plans. Echinoderms are thought to have evolved from a bilateral ancestor[1]. Therefore, the developmental process forming the pentaradial symmetry is an important issue to understand the diversification of animal forms[2], although the developmental mechanisms underlying the establishment of the pentaradial body plan remain to be elucidated[3].

In both extant and fossil species, the primary body axis of echinoderms is defined based on the arrangement of the ambulacrum, a region associated with the water vascular system[4]. The water vascular system is a synapomorphy of echinoderms that is involved in locomotion, circulation and feeding. The water vascular system exhibits a pentaradial structure forming a tubular network consisting of a ring canal around the mouth and radial canals that extend from the ring canal[5]. Thus, the water vascular system is an essential key character for considering the echinoderm body plans[6].

The water vascular system is formed from the hydrocoel, i.e., a mesodermal coelom that emerges on the left side of a bilateral larva[5,7]. In echinoderms, bilateral larvae are transformed into juveniles with pentaradial body plans through metamorphosis. At the time of metamorphosis, multiples of five buds (hydrocoel lobes) are projected from the hydrocoel, and the whole hydrocoel encircles the mouth, forming a ring and resulting in a pentaradial water vascular system (Fig. 1). It is known that in many echinoderm species the emergence of a multiple of five lobes on the hydrocoel is the first pentameral character in the ontogeny. The outline of the hydrocoel development has so far been described in many echinoderms, and recent advances in microscopy enable us to observe the detailed structures inside an embryo[8]. However, the morphogenetic mechanisms underlying the hydrocoel formation, especially histological transitions and behaviors of hydrocoel cells, have not yet been unraveled.

Although many of the studies on echinoderm development have been carried out in sea urchins as the study materials[9], no studies have so far been conducted on the morphogenetic processes of hydrocoel-lobe formation in sea urchins due to their biological characteristics. For example, in *Strongylocentrotus purpuratus* showing indirect development, it takes a month from fertilization to the hydrocoel-lobe formation and its hydrocoel overlaps with the vestibule invagination which contributes to the adult rudiment[10], making observations on the hydrocoel difficult. On the other hand, sea cucumbers (Holothuroidea) such as *Apostichopus japonicus*, showing indirect development, are suitable models to observe hydrocoel development, since their larva is transparent and does not form the hydrocoel-associated structures such as the adult rudiment, so the hydrocoel-lobe formation is easily observable.

The hydrocoel of *A. japonicus* is formed from the archenteron on the left side of the auricularia larva around 4 days post-fertilization (dpf). The larvae develop relatively quickly as indirect developers, so the hydrocoel lobes are formed on the hydrocoel approximately 10 dpf[11,12]. In this species, as in other holothurians, 10 hydrocoel lobes are formed on the hydrocoel. Five major lobes (I-V) develop into water vascular canals of tentacles. Another five minor lobes (i-v), which are formed between each of the major lobes, extend posteriorly and develop into radial canals of the water vascular system (Fig. 1b)[13,14]. The hydrocoel becomes horseshoe-like shaped after the lobe formation and then forms the ring canal surrounding the digestive tract to establish the pentaradial structure. At the same time of ring canal formation, metamorphosis starts and the whole larval body is rearranged to become a doliolaria larva.

After the hydrocoel-lobe formation, pentaradial structures of adult sea cucumber such as longitudinal muscle bands and radial nerve cords are formed along the radial canals, which are formed from hydrocoel lobes[15,16,17]. Other echinoderms such as sea urchins also form pentaradial adult tissues around the hydrocoel[5], which suggests that the hydrocoel lobes might induce the formation of pentaradial structures of echinoderms and contribute to the establishment of the pentaradial body axis also in these species. Thus, the spatial control of hydrocoel lobe formation and the determination of the number of hydrocoel lobes is thought to be critical to the development of the pentaradial body plan.

In general, histological changes during morphogenesis involve changes in cell number, cell shape and cell arrangement[18]. In particular, branching or budding morphogenesis is driven by the contribution of cell proliferation and collective migration to the morphogenesis[19]. Therefore, it was considered that either, or both, of these cellular processes should be involved in the hydrocoel-lobe formation.

In this study, therefore, to reveal the morphogenetic process underlying the hydrocoel lobe formation in *A. japonicus*, detailed observations at the cellular level were carried out focusing on changes in cell proliferation and cell arrangement during the formation process.

Methods

Animals

Mature adults of *A. japonicus* were collected between April and June of 2019-2021 from sandy bottom of the sea at the depth of 3-10 m around the Misaki Marine Biological Station, Kanagawa or at Onahama Port, Fukushima (36° 94' N, 140° 90' E) by SCUBA diving. All the collected individuals were morphologically diagnosed as the black type of the focal species, that was recently redescribed as *A. armatus*[31] although it is still treated as *A. japonicus* in many recent studies. Collected individuals were kept in the laboratory tank at 17 ºC to maintain the sexually mature condition. Gonads of collected individuals were dissected from inside the body wall to discriminate sex and maturity. Mature ovary is vivid orange and mature testis is white. Egg spawning was induced by the injection of 500 µL of 10 µM cubifrin (Kyusyu TLO Company, Fukuoka, Japan), a peptide known to induce oocyte maturation and spawning in *A. japonicus*[32]. Sperms were obtained by dissecting matured testes in sea water.

Embryo culture was conducted based on Kikuchi et al.[33] . Briefly, embryos were kept in 10 L of filtered sea water in a plastic container with circulation at 20 ºC, and daily fed *Chaetoceros calcitrants* diatoms. The density of individuals was kept as 1 embryo/mL, and sea water was changed every two days. Embryos become bilateral auricularia larva at 2 dpf. The hydrocoel emerges at the left side of the digestive tract around 6 dpf and the hydrocoel lobes can be observed around 10 dpf[11]. Individuals during this period were used for observations. After the formation of hydrocoel lobes, larvae metamorphose into doliolaria and pentactula juveniles, and settle down on the container bottom.

Morphological observation of the hydrocoel

For observations of the overall shape of hydrocoel, larvae were fixed using Fix1 (4% PFA/ 0.1M MOPS, pH 7.0/ 0.5M NaCl)[33]). Specimens were stained with DAPI (Nakalai Tesque, Kyoto, Japan) for observation of the overall morphology of the hydrocoel. For observations of cell arrangements and cell shapes, *N*-(4,4-Difluoro-5,7-Dimethyl-4-Bora-3a,4a-Diaza-s-Indacene-3-Pentanoyl) Sphingosine (BODIPY FL C_5-Ceramide) (Life Technologies, Carlsbad, CA, USA) was used. Larvae were kept alive in BODIPY FL C_5-Ceramide 100 µM in sea water, for 6 hours at 20 °C. Based on a previous study[34], specimens were embedded on the glass bottom dish using 1% low temperature melting agarose. The specimens were then observed using a confocal laser scanning microscope FV3000, Olympus, Tokyo, Japan and an optical microscope (TE300 Nikon, Tokyo, Japan) equipped with a camera (DP27, Olympus, Tokyo, Japan).

Detection and inhibition of cell proliferation

To observe the localization of cell proliferation, the intake of thymidine analogue 5-ethynyl-2'-deoxyuridine (EdU) was detected using a Click-iT^{TM} EdU Cell Proliferation Kit for Imaging (Life Technologies, Eugene, OR, USA). EdU labeling was conducted based on Sharma & Ettensohn[35] with some modifications. EdU was diluted to 10 µM in filtered sea water according to the manufacturer's instruction. Auricularia larvae at each phase were incubated in 10 mL of EdU sea water for 3 hours at 20 ºC. Larvae were fixed with Fix1 soon after the treatment. Detection of EdU was conducted based on the manufacturer's instructions and cell nuclei were stained with DAPI. Then, the stained specimens were observed using a confocal laser scanning microscope.

Cell proliferation was inhibited using DNA polymerase I inhibitor aphidicolin (Adipogen, Liestal, Switzerland). This reagent is known to inhibit cell proliferation in a sea urchin, *Lytechinus pictus*[36], as in many other eukaryotes. The treatment method was based on Smith et al.[21] . Aphidicolin was dissolved at a concentration of 10 mg/ml in dimethyl sulfoxide (DMSO) and diluted to 0.5 µl/ml in filtered sea water. Auricularia larvae before lobe formation were incubated in aphidicolin sea water for 20 hours at 20 ºC. Control experiments were conducted by incubating in the same condition using 0.5 µl/ml DMSO in filtered sea water. For the evaluation of the effect of aphidicolin on the hydrocoel lobe formation, phase 2 larvae were randomly divided into 6 groups. 3 of the groups were kept in aphidicolin sea water and the other 3 groups were kept in DMSO sea water (control). Larvae were fixed after 20 h treatment and the number of larvae which formed the hydrocoel lobes (phase 3 and phase 4) were counted (10-18 larvae in each group). Two-sided Fisher's exact test was carried out with R 4.0.3.

Results

Staging of hydrocoel lobe formation

Firstly, the overall process of hydrocoel-lobe formation in auricularia larvae was observed, focusing on morphological characteristics. Fixed specimens were observed under an optical microscope and a confocal laser scanning microscope after staining with 4',6-Diamidino-2-phenylindole (DAPI) (Fig. 2). During the formation process, 4 developmental phases were defined based on the hydrocoel morphology (Table 1).

Phase 1: The hydrocoel primarily emerged at the left side of the digestive tract, showing a spindle-like shape (Fig. 2a-a‴).

Phase 2: The entire hydrocoel extended up to 100 µm along its longitudinal axis of the spindle shape and became a slightly curved columnar shape (Fig. 2b-b‴).

Phase 3: The hydrocoel lobes started to form (Fig. 2c-c‴). The lobes were formed in a line along the AP axis of a larva. Each of 5 minor hydrocoel lobes which will become radial water vascular canals were respectively formed between the 5 major hydrocoel lobes which became water vascular canals of tentacles.

Phase 4: The lobes continuously extended to form tubular structures (Fig. 2d-d‴). Each hydrocoel formed a tubular structure surrounded by epithelial tissue, and these tubular structures later formed the tubular network of the water vascular system.

There were no other obvious morphological changes in other parts of an auricularia larva, such as the digestive tract and ciliate bands, throughout these phases.

Observations of cell proliferation

To examine whether cell proliferation contributes to the hydrocoel morphogenesis, we observed the distribution patterns of cell-proliferation signals by labelling with 5-Ethynyl-2'-deoxyuridine (EdU) during the process. Larvae were incubated in 10 μM EdU sea water for 3 hours. In all of the observed phases, cell proliferation was detected (Fig. 3).

In phases 1 and 2, the EdU signal was distributed throughout the whole hydrocoel, and observations of both z-stack images and optical sections indicated that the signal was equally localized throughout the hydrocoel (Fig. 3a-b, a'-b"). The cell proliferation was also observed in phases 3 and 4 (Fig. 3 c-d, c'-d'). Both z-stack images and optical sections showed that the EdU signals were not specifically localized at certain regions including lobe tips (Fig. 3c-d, c'-d', arrowheads).

To examine whether cell proliferation is required for the hydrocoel-lobe formation, larvae at phase 2 was treated with the cell proliferation inhibitor aphidicolin. Administration of 0.5 μg/mL aphidicolin was shown to completely inhibit the EdU incorporation into the hydrocoel tissues, confirming the effect of aphidicolin (Fig. S1). Then auricularia larvae at phase 2, just prior to the hydrocoel-lobe formation, were treated with 0.5 μg/ml aphidicolin (Fig. 4a). At 20 hours after the onset of treatment, the hydrocoel lobes were successfully formed, as in untreated animals (Fig. 4b). There was no significant difference in the ratio of larvae in which hydrocoel lobes were formed (phase 3 or 4) to larvae in which hydrocoel lobes were not formed yet (phase 2) between the treated and control groups (Two-sided Fisher's exact test, $p = 0.144$, Fig. 4c).

Observations on cell arrangement

To observe the changes of cell shape and cell arrangement in the hydrocoel epithelium, the cell membrane of live larvae was stained with bodipy FL C5-ceramide. At phase 1, the hydrocoel was surrounded by a single layer of columnar epithelial cells (Fig. 5a). At phase 2, the hydrocoel epithelium was stratified, which was observed throughout the whole hydrocoel (Fig. 5b). At phase 3, when the lobe formation started, stratified epithelial tissue became single-layered epithelium again at the tip of the hydrocoel lobes (Fig. 5c-d). The tissue between the lobes was still multi-layered and started to be bent. At phase 4, when the hydrocoel lobes extended, the epithelium between the lobes also became single-layered, being sharply bent, and consequently the lobe shape became more constricted (Fig. 5e-f).

The positions of hydrocoel lobes were the same in all of the observed individuals, and all of the hydrocoel lobes formed synchronously (Fig. 5). Although the lobes for water vascular canals of tentacles (i.e., lobe I, II, III, IV and V) were relatively larger than those for radial canals (i.e., lobe ii, iii, and iv) except for lobe i, the transitions in cell arrangement from multi-layered to monolayered epithelium were observed in all of the lobes regardless of lobe size (Fig. 5, 6).

Discussion

In general, developmental mechanisms of the formation of branching or budding structures in the epithelium can be classified into 3 categories, i.e., single cell extension, collective migration and non-

migratory branching[19]. Since the hydrocoel lobes are multicellular structures, the mechanism underlying the hydrocoel morphogenesis should be driven by cell migration or non-migratory mechanisms. The non-migratory branching is typically observed during the morphogenesis of vertebrate kidney and mammalian lung[19]. The morphogenesis of ureteric buds in kidney is driven by localized proliferation at the tip of the branch[19]. In the hydrocoel-lobe formation, cell proliferation was evenly distributed throughout the hydrocoel, and no specific localization of proliferation, such as concentration at hydrocoel-lobe tips, was observed in relation to the lobe formation (Fig. 3b, c). It is still possible that cell proliferation drives the formation of hydrocoel lobes even if no specific localization of cell proliferation was detected. In the case of lung branching in mammals, global proliferation drives the budding process in coordination with cell shape change and localized muscle cell differentiation[19]. In the hydrocoel-lobe morphogenesis, however, cell proliferation seems to be unnecessary for the hydrocoel-lobe budding, since the inhibition of cell proliferation during phase 2 and phase 4 did not prevent the lobe formation (Fig. 4).

A previous research in a direct-developing sea urchin, *Heliocidaris erythrogramma*, showed that the cell proliferation is not necessary for the formation of the hydrocoel itself[20]. In the hydrocoel formation in *A. japonicus*, however, the stratification and the successive intercalation of epithelial cells are suggested to be driving forces for the hydrocoel morphogenesis. On the other hand, since cell proliferation is known to be required for the stratification of epithelium[21], the cell proliferation between phase 1 and 2 is suggested to contribute indirectly to the hydrocoel lobe morphogenesis.

Based on our observations on cell shape and cell arrangement in the hydrocoel, intercalation of epithelial cells is suggested to contribute to budding morphogenesis in the hydrocoel-lobe formation. At phase 1, the hydrocoel epithelium consisted of a single-layered cell sheet, but then it was stratified at phase 2 (Fig. 5). Multi-layered epithelial cells became single-layered arrangement again specifically at the lobe-tip position (phase 3, Fig. 5). This change in cell arrangement is supposed to be achieved by cell intercalation. After the tip intercalation and the lobe extension, intercalation occurred at the proximal part of each lobe, (phase 4, Fig. 5). This time-dependent difference of cell intercalation depending on the positions in the hydrocoel lobes suggests that the cell intercalation occurs sequentially from the tip of the hydrocoel lobe to the proximal part. Cell intercalation observed in these phases can be categorized as “radial intercalation”, in which cells intercalated in the direction perpendicular to the epithelium and the multiple cell layers were transformed into a single layer[22]. Radial intercalation is thought to leads to tissue spreading[23], so the tissue expansion caused by the sequential radial intercalation might contribute to budding and elongation of hydrocoel lobes. Thus, the radial cell intercalation seems to be involved in the morphogenetic process of hydrocoel lobes, and it can be said that the morphogenetic process of hydrocoel lobes consist of branching driven by cell migration though further testing such as inhibition of cell migration is needed. In addition, the tissue was curved sharply at the tips of hydrocoel lobes and between the hydrocoel lobes as the hydrocoel lobes developed, although it is not clear whether these changes in epithelial tissue constitute an active process to form the hydrocoel lobes or a passive result of morphogenetic processes such as cell intercalation.

The result of this study is the first report suggesting the involvement of radial intercalation in echinoderm development. In the sea urchin *Lytechinus pictus*, in which cell behavior during gastrulation has been well studied, it is known that the cell-shape change and the convergent extension caused by mediolateral intercalation are involved in gastrulation[24,25,26], while stratification and radial intercalation should not be involved, since the archenteron is single-layered epithelium in this species. In the branching morphogenesis of the mouse mammary gland, it is known that simple epithelium becomes transiently stratified and is then resolved to simple epithelium again to form the branching structure[27], and tube elongation is achieved by radial intercalation[23]. Hydrocoel-lobe morphogenesis resembles these processes. On the other hand, indispensable structures in mammary ductal elongation such as the myoepithelium which covers the ducts[23] or the growth zone like terminal end bud, which is stratified and shows a high proliferation rate[28,29] were not observed in the sea cucumber hydrocoel.

It is known that radial intercalation is driven by cell chemotaxis in amphibian epiboly[30]. Therefore, in the focal sea cucumber, sequential radial intercalation during the hydrocoel-lobe formation could also be driven by chemotaxis. If so, the diffusion pattern of attractants and/or the localization of their source might determine the number and the position of hydrocoel lobes. Alternatively, specific localization of gene expression might regulate the responsiveness of epithelial cells to the attractants, leading to the sequential intercalation. Future studies on the molecular mechanisms involved in hydrocoel-lobe morphogenesis will help us to understand the developmental mechanisms underlying the pentaradial body plans in echinoderms.

Declarations

Acknowledgement

We would like to express our gratitude to Y. Harumoto and the staff of Aquamarine Fukushima, Fukushima Ocean Science Museum, the staff of Miura Fishery Cooperative, the staff of Kanagawa Prefectural Marine Science Senior High School, and M. Sekifuji, M. Kawabata and M. Kyokuwa for assisting us at the time of sampling. M. Yoshida, D. Kurokawa, M. Okanishi, N. Irie, T. Kawanishi and H. Takeda provided us a number of constructive comments on the current study. Thanks are also due to Elizabeth Nakajima for English editing. This work was supported by a Grant-in-Aid for Scientific Research A (No. 18H04006) to TM, a Grant-in-Aid for JSPS Fellows to SU (no. 21J11134) and the World-leading Innovative Graduate Program for Life Science and Technology from the Ministry of Education, Culture, Sports, Science and Technology of Japan.

Author Contributions

SU and TM designed the whole study. SU and HK collected the study materials from the field. SU reared animals and observed the developmental processes. SU, KO and TI performed the experimental procedures. All the authors wrote the manuscript.

References

1. Smith, A. B., Peterson, K. J., Wray, G. & Littlewood, D. T. J. From Bilateral Symmetry to Pentaradiality: The Phylogeny of Hemichordates and Echinoderms. in *Assembling the Tree of Life* (eds. Cracraft, J., Donoghue, M. J. & Editors) 365–383 (Oxford University Press, 2004).
2. Raff, R. A. *The Shape of Life.* (The University of Chicago Press, Chicago., 1996).
3. Byrne, M., Martinez, P. & Morris, V. Evolution of a pentameral body plan was not linked to translocation of anterior Hox genes: The echinoderm HOX cluster revisited. *Dev.***18,** 137–143 (2016).
4. Sumrall, C. D. & Wray, G. A. Ontogeny in the fossil record: diversification of body plans and the evolution of “aberrant” symmetry in Paleozoic echinoderms. *Paleobiology***33,** 149–163 (2007).
5. Hyman, L. H. *The Invertebrates: Echinodermata, the Coelomate Bilateria*. Volume IV. (1955).
6. Rozhnov, S. V. Symmetry of echinoderms: From initial bilaterally-asymmetric metamerism to pentaradiality. *Sci.***06,** 171–183 (2014).
7. Omori, A., Kikuchi, M. & Kondo, M. Larval and Adult Body Axes in Echinoderms. in *Reproductive and Developmental Strategies* (eds. Kobayashi, K., Kitano, T., Iwao, Y. & Kondo, M.) 763–789 (Springer, 2018). doi:10.1007/978-4-431-56609-0_34.
8. Morris, V. B. Analysis of coelom development in the sea urchin *Holopneustes purpurescens* yielding a deuterostome body plan. *Open***5,** 348–358 (2016).
9. Cary, G. A. & Hinman, V. F. Echinoderm development and evolution in the post-genomic era. *Biol.***427,** 203–211 (2017).
10. Smith, M. M., Smith, L. C., Cameron, R. A. & Urry, L. A. The larval stages of the sea urchin, *Strongylocentrotus purpuratus. J. Morphol.***269,** 713–733 (2008).
11. Yoshida, W., Tamai, A., Yanaka, T. & Ishida, S. Normal development and artificial breeding of sea cucumber (*Stichopus japonicus* Selenka) from Mutsu Bay. *Fac. Agric. Life Sci., Hirosaki Univ*. **4,** 16–23 (2001).
12. Qiu, T., Zhang, T., Hamel, J. F. & Mercier, A. Development, Settlement, and Post-settlement Growth. *Aquac. Fish. Sci.***39,** 111–131 (2015).
13. Smiley, S. Metamorphosis of *Stichopus californicus* (Echinodermata: Holothuroidea) and its phylogenetic implications. *Bull.***171,** 611–631 (1986).
14. Smirnov, A. V. Sea cucumbers symmetry (Echinodermata: Holothuroidea). *J.***48,** 1215–1236 (2014).
15. Dolmatov, Y. I. & Ivantey, V. A. Histogenesis of Longitudinal Muscular Bands in a Holothrian. *J. Dev. Biol.***24,** 401–405 (1993).
16. Mashanov, V. S., Zueva, O. R., Heinzeller, T., Aschauer, B. & Dolmatov, I. Y. Developmental origin of the adult nervous system in a holothurian: an attempt to unravel the enigma of neurogenesis in echinoderms. *Dev.***9,** 244–256 (2007).
17. Dolmatov, I. Y., Ginanova, T. T. & Frolova, L. T. Metamorphosis and definitive organogenesis in the holothurian *Apostichopus japonicus*. *Zoomorphology***135,** 173–188 (2016).

18. Heisenberg, C. P. & Bellaïche, Y. Forces in tissue morphogenesis and patterning. *Cell***153,** 948 (2013).
19. Spurlin, J. W. I. & Nelson, C. M. Building branched tissue structures: from single cell guidance to coordinated construction. *Trans. R. Soc. B*. **372,** 20150527 (2017).
20. Smith, M. S., Collins, S. & Raff, R. A. Morphogenetic mechanisms of coelom formation in the direct-developing sea urchin Heliocidaris erythrogramma. *Genes Evol.***219,** 21–29 (2009).
21. Li, J., Chatzeli, L., Panousopoulou, E., Tucker, A. S. & Green, J. B. A. Epithelial stratification and placode invagination are separable functions in early morphogenesis of the molar tooth. **143**, 670–681 (2016).
22. Keller, R. E. The cellular basis of epiboly: An SEM study of deep-cell rearrangement during gastrulation in Xenopus laevis. *Embryol. Exp. Morphol.***60,** 201–234 (1980).
23. Neumann, N. M. et al. Coordination of Receptor Tyrosine Kinase Signaling and Interfacial Tension Dynamics Drives Radial Intercalation and Tube Elongation. *Cell***45,** 67-82 (2018).
24. Ettensohn, C. A. Gastrulation in the sea urchin embryo is accompanied by the rearrangement of invaginating epithelial cells. *Biol*. **112,** 383–390 (1985).
25. Hardin, J. D. & Cheng, L. Y. The mechanisms and mechanics of archenteron elongation during sea urchin gastrulation. *Biol*. **115,** 490–501 (1986).
26. Kimberly, E. L. & Hardin, J. Bottle cells are required for the initiation of primary invagination in the sea urchin embryo. *Biol.***204,** 235–250 (1998).
27. Ewald, A. J. et al. Mammary collective cell migration involves transient loss of epithelial features and individual cell migration within the epithelium. *Cell Sci.***125,** 2638–2654 (2012).
28. Hinck, L. & Silberstein, G. B. The mammary end bud as a motile organ. *Breast Cancer Res.***7,** 245–251 (2005).
29. Williams, J. M. & Daniel, C. W. Mammary ductal elongation: Differentiation of myoepithelium and basal lamina during branching morphogenesis. *Biol.***97,** 274–290 (1983).
30. Szabó, A. et al. The Molecular Basis of Radial Intercalation during Tissue Spreading in Early Development. *Cell***37,** 213–225 (2016).
31. Woo, S. P. et al. A taxonomic revision of the genus Apostichopus (Holothuroidea: Stichopodidae) from Japan. *Zootaxa* **4350,** 121–135 (2017).
32. Kato, S. et al. Neuronal peptides induce oocyte maturation and gamete spawning of sea cucumber, Apostichopus japonicus. *Biol.***326,** 169–176 (2009).
33. Kikuchi, M., Omori, A., Kurokawa, D. & Akasaka, K. Patterning of anteroposterior body axis displayed in the expression of Hox genes in sea cucumber Apostichopus japonicus. *Genes Evol.***225,** 275–286 (2015).
34. Vidavsky, N. et al. Calcium transport into the cells of the sea urchin larva in relation to spicule formation. *Natl. Acad. Sci. U. S. A.***113,** 12637–12642 (2016). Vidavsky et al., 2016

35. Sharma, T. & Ettensohn, C. A. Regulative deployment of the skeletogenic gene regulatory network during sea urchin development. *Development***138,** 2581–2590 (2011).
36. Stephens, L. The Effects of Aphidicolin on Morphogenesis and Differentiation in the Sea Urchin Embryo. *Biol.***118,** 64–69 (1986).

Tables

Table 1 Features of hydrocoel tissue in each phase of the hydrocoel lobe morphogenesis.

phase	Feature
phase 1	• Spindle shape (hydrocoel lobes are not formed.) • Single layered cell sheet
phase 2	• Bean shape (hydrocoel lobes are not formed) • Stratified cell sheet
phase 3	• Emergence of the hydrocoel lobe • Single layered at the tip of the hydrocoel lobes
phase 4	• Extension of the hydrocoel lobe • Single layered in the entire hydrocoel lobes

Figures

Figure 1

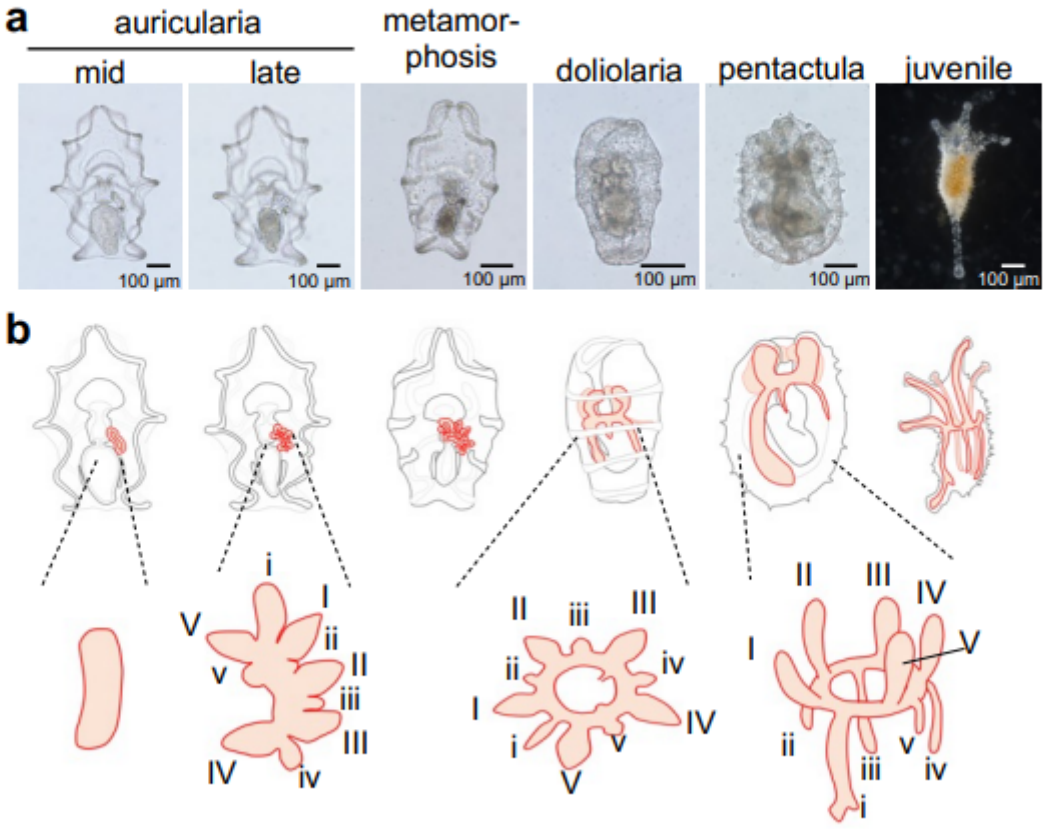

Figure 1

Normal development of the sea cucumber Apostichopus japonicus and schematic illustration of its hydrocoel. (a) The developmental process during auricularia larva and juvenile stages. Development proceeds from left to right. Auricularia, doliolaria, metamorphosis and pentactula are ventral views, anterior top, and juvenile is dorsal view, anterior top. (b) Schematic illustration of hydrocoel in each developmental stage. Orange part represents the hydrocoel or its derivative, i.e., the water vascular system. Auricularia, and metamorphosing larva are ventral views and doliolaria, pentactula and juvenile are left lateral views, anterior top. The hydrocoel emerges on the left side of the archenteron in an auricularia, and ten lobes are formed from the hydrocoel. After the lobe formation, the hydrocoel become horseshoe-like shaped to form a ring canal surrounding the digestive tract. Then, the larva metamorphoses into a doliolaria. Five of the lobes (I-V) extend anteriorly and become the water vascular canal of the tentacle of a juvenile and another five lobes (i-v) formed between the water vascular canals of the tentacle extend posteriorly and become radial canals. The numbering identities for hydrocoel lobes are based on Loven's axis to sea cucumbers14.

Figure 2

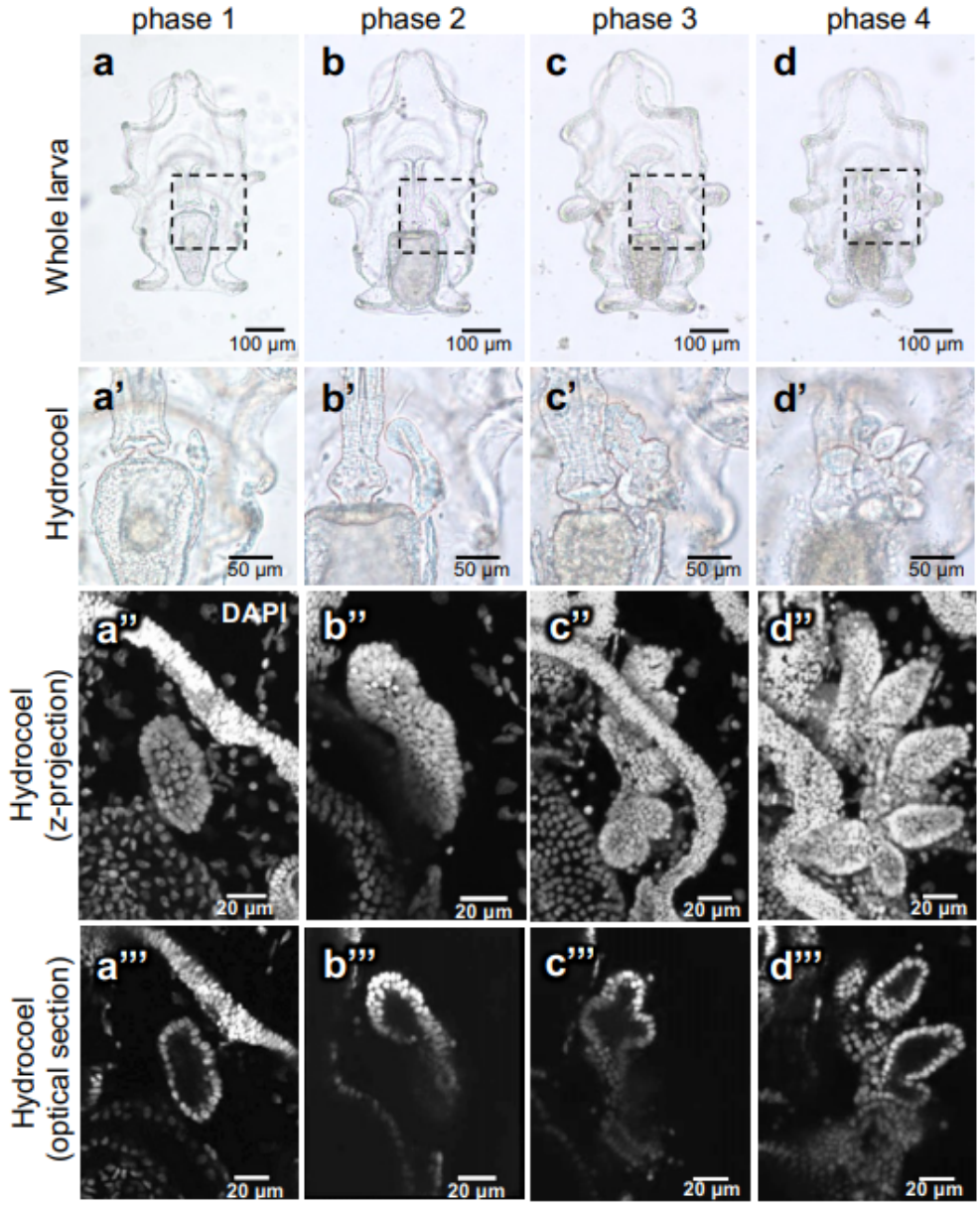

Figure 2

Observation of the overall morphology of the developing hydrocoel lobes. . (a-d) show the whole embryo under the microscope (ventral view, anterior top) from phase 1 to phase 4. (a'-d') show the hydrocoel of a-d. The dotted lines in (a-d) indicate the region shown in (a'-d'). The hydrocoel of the specimens stained with DAPI are shown in (a"-d': z-stack images) and (a"'-d"': optical sections). In phase 1, the hydrocoel was spindle shaped and then it extended up to 100 µm along the longitudinal axis in phase 2. The hydrocoel

lobes started to form in phase 3 and the lobes extended in phase 4. During phase 1 and phase 4, no significant change in the overall morphology of entire larva other than the change in the hydrocoel was observed.

Figure 3

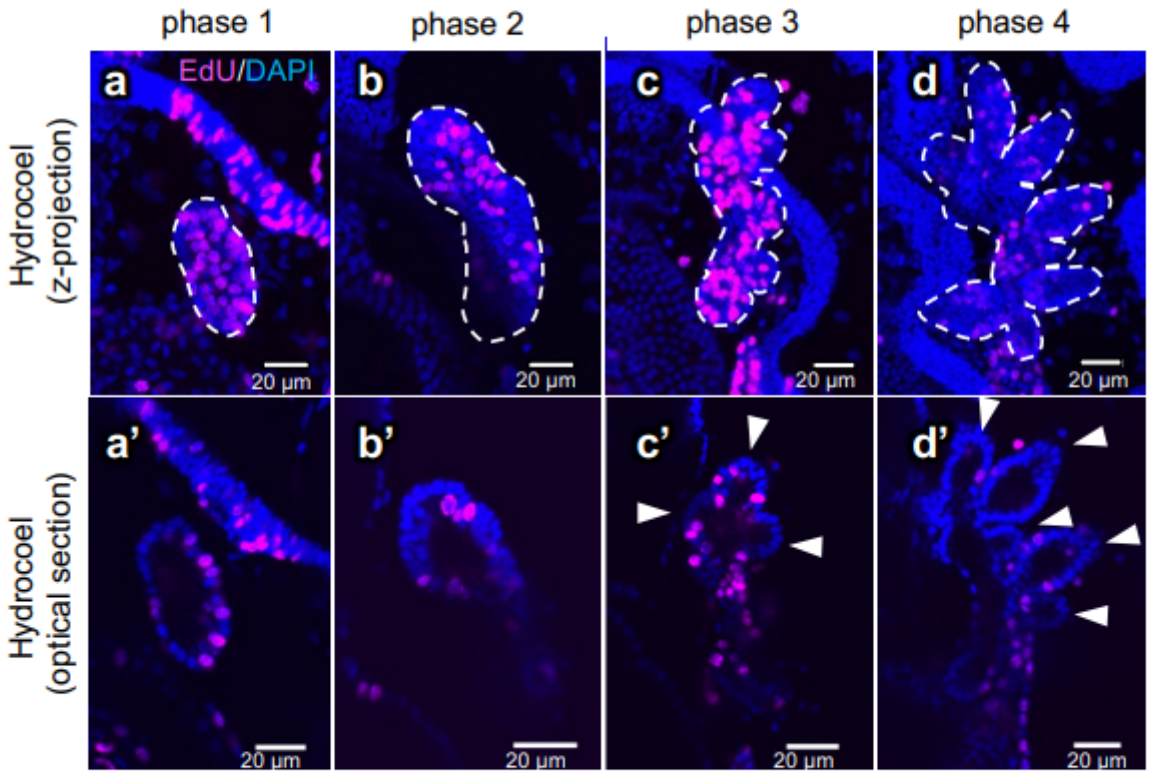

Figure 3

The spatial distribution of cell proliferation in the hydrocoel during the hydrocoel lobe morphogenesis. The cell proliferation in the hydrocoel from phase 1 to phase 4 was detected using EdU after a 3-hour EdU treatment (a-d). The hydrocoel is indicated by the dotted lines. (a'-d') show the optical sections of a-c. The

position of the hydrocoel lobe is indicated by arrowheads. The EdU signal was detected equally throughout the whole hydrocoel during phase 1 and phase 4 and specific localization was not observed.

Figure 4

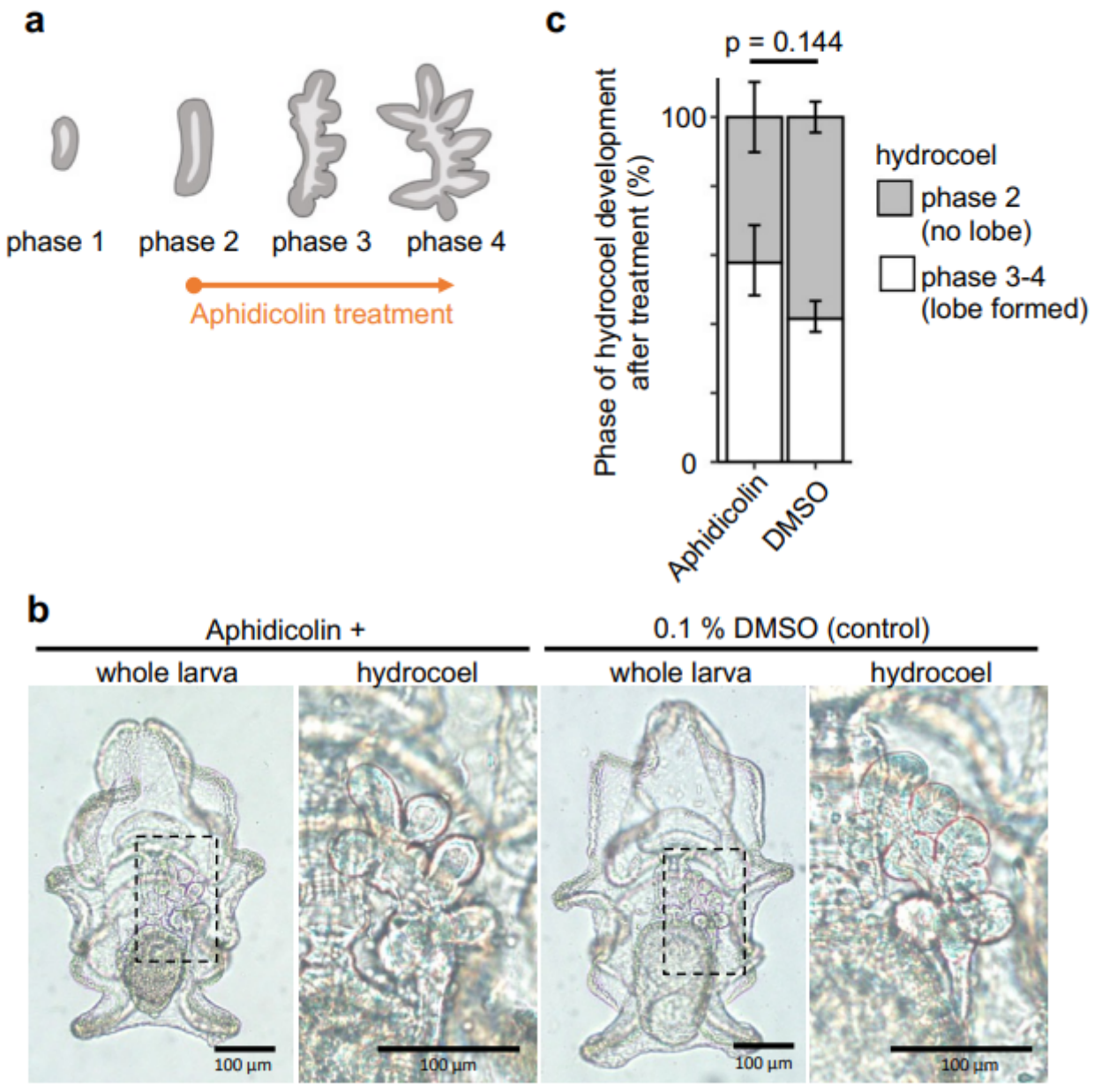

Figure 4

Inhibition of cell proliferation by aphidicolin treatment during the hydrocoel lobe morphogenesis. (a) Experimental design for aphidicolin treatment. Auricularia larvae were treated with aphidicolin beginning at phase 2 and the phenotype was observed at 20 hours. (b) Phenotype resulting from aphidicolin

treatment. Hydrocoel lobe was formed both in aphidicolin treatment and DMSO treatment (control) larvae. The number or shape of hydrocoel lobes (arrowhead) was not affected by the aphidicolin treatment compared to DMSO treatment. (c) Ratio of phase 3-4 larva (lobe formed) to phase 2 larva (lobe not formed)in treated and control groups at 20 h after the initiation of treatment. There was no significant difference (Student's t-test, p = 0.06457). Graph represents the mean ± s.d. from 3 independent experiments.

Figure 5

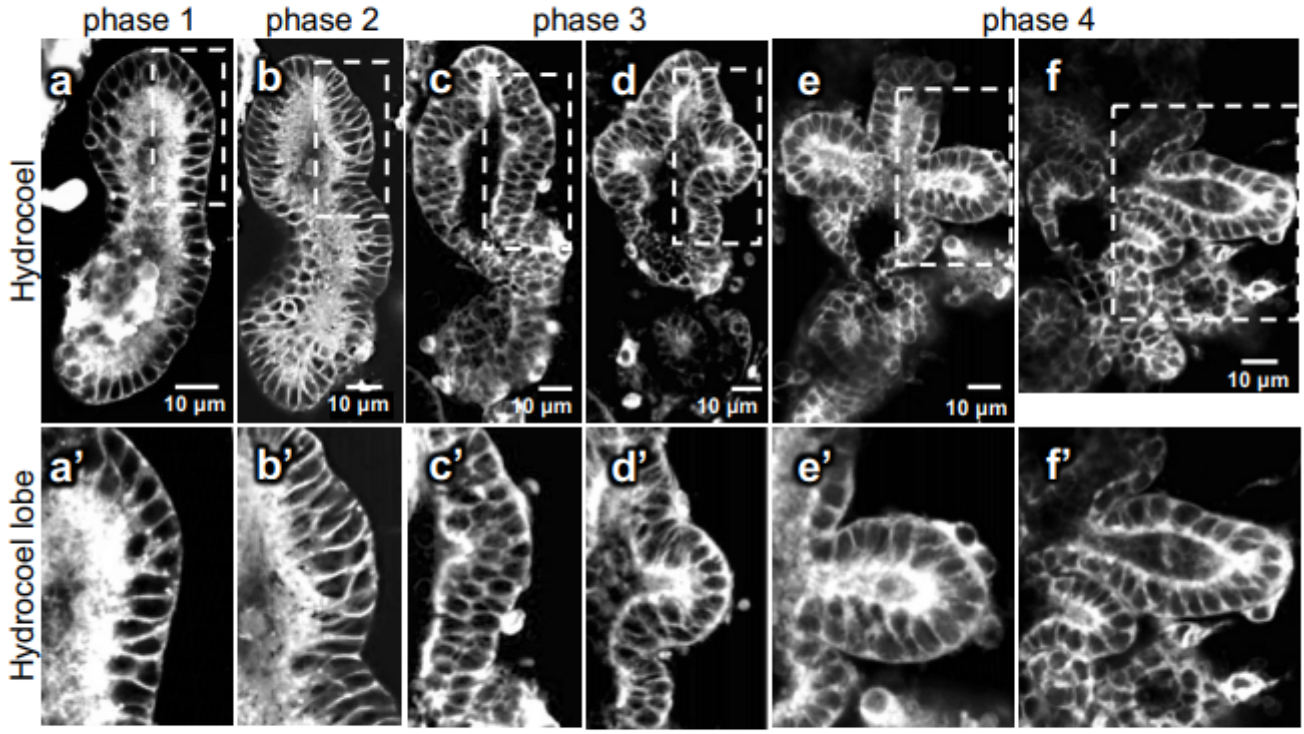

Figure 5

The observed changes in cell shape and cell arrangement during the lobe formation in the hydrocoel. Cell membrane of larvae was stained by BODIPY FL C5-Ceramide and observed using confocal laser scanning microscopy from phase 1 to phase 4. (a-f) are optical sections of the hydrocoel in each phase (ventral view, anterior top). The time-course and stages are indicated in the figure. (a'-f') show the magnification of regions indicated in (a-f), respectively. Hydrocoel epithelium was a single cell layer in

phase 1 and then became stratified in phase 2. In phase 3, the tissue became single layered again at the tip of the lobe (arrowhead in C'-D') and then in the whole hydrocoel lobe.

Figure 6

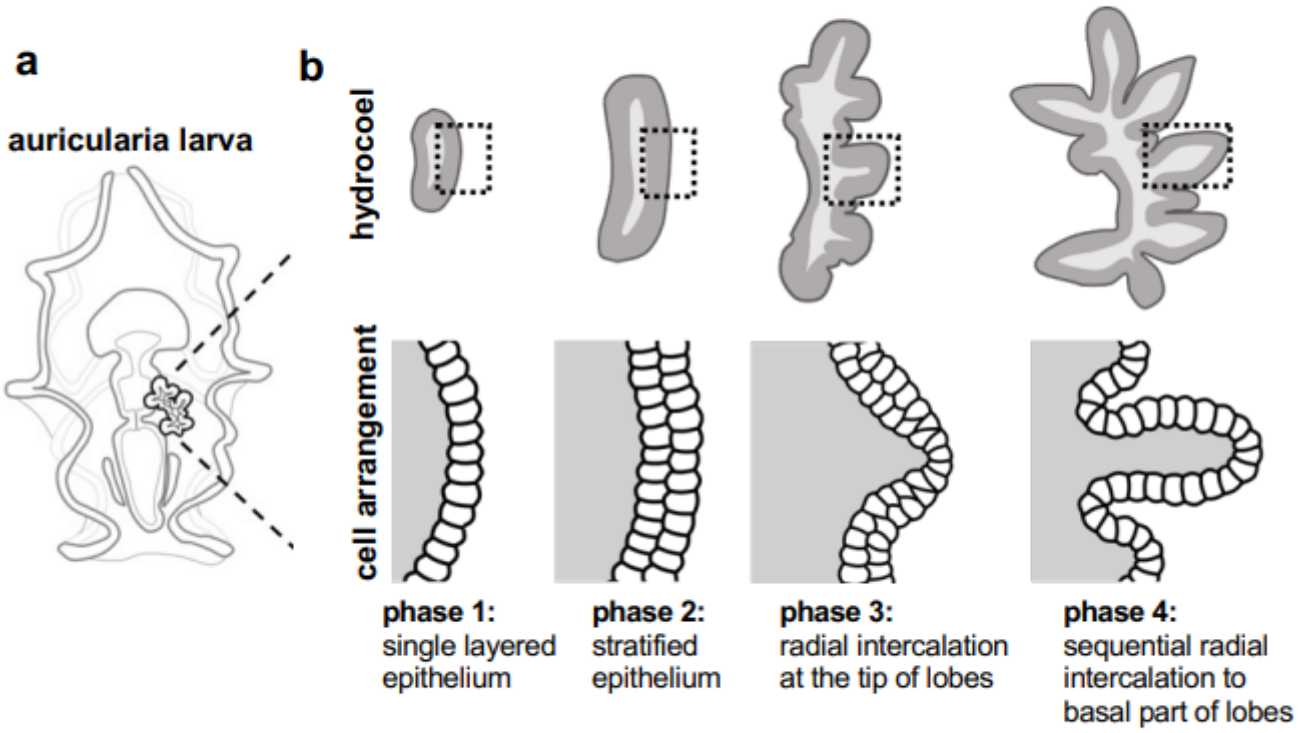

Figure 6

Schematic illustration of change in cell arrangement during the hydrocoel lobe morphogenesis. (a) represents an auricularia larva and (b) represents the development of its hydrocoel. Upper panel is the overall shape of the hydrocoel, and the cell arrangement of hydrocoel epithelium in dotted areas is shown in the lower panel. The hydrocoel at phase 1 consists of a single cell sheet, and it becomes stratified at phase 2. As the formation of the hydrocoel lobe proceeds, the cell sheet becomes single layered again sequentially from the tip of the hydrocoel lobe (phase 3) to the proximal part of the lobe (phase 4).

Supplementary Files

This is a list of supplementary files associated with this preprint. Click to download.

- SupplemntaryFigure211203.pdf